Computing component requirements for multiple connected transfer paths of structural borne noise

D. Xu [1], M. Häußler [2], M. Zimmermann [1]
[1] Technical University of Munich, TUM School of Engineering and Design,
Laboratory for Product Development and Lightweight,
Boltzmannstr. 15, 85748, Garching, Germany

[2] VIBES.technology,
Molengraaffsingel 14, 2629 JD, Delft, The Netherlands

Abstract
Reducing noise propagation in mechanical structures can be difficult when several components on multiple intersecting transfer paths interact. One way to reduce design complexity caused by the transfer path interaction is to derive component requirements from the system design goal. The component requirements should ensure that the system design goal is reached whenever these requirements are met. In this paper, we present an approach that computes solution-neutral requirements on isolation elements of multiple connected transfer paths, such that each of them can be developed independently and efficiently. This is accomplished by first modeling the system dynamics with Dynamic Substructuring and Transfer Path Analysis. Secondly, the ranges of admissible stiffness of isolation elements are quantitatively expressed as a so-called solution space for each isolation element. The proposed approach is applied to the noise propagation path of an electric compressor in a passenger vehicle.

1 Introduction

Two types of noise are typically distinguished, air-borne and structure-borne noise. Structure-borne noise is more dominant in the lower frequency range (approximately lower than 1000 Hz), while air-borne noise is mainly perceived by humans in a rather high frequency range [1]. The excitation of the *source structure* is propagated through the *transfer path* and perceived by the *receiver* (see Figure 1 (a)). While the transfer path of air-borne noise is rather straightforward [2], the transfer path of structure-borne noise could be much more complex. This is not only because a transfer path could consist of many components, which could be seen as a *transfer chain* (see Figure 1 (b)). Multiple transfer paths could also exist (see Figure 1 (c)). More importantly, the transfer paths have complex interactions with each other, which turns a complex mechanical system (the passenger car as an example in the scope of this research) into a *transfer network* for structure-borne noise (see Figure 1 (d)). This raises the complexity of the noise propagation problem and makes it difficult to find effective measures for noise reduction.

To simplify the design of a complex system, it is commonly desired to break the development of a whole system into smaller design tasks that are much easier to solve. According to the V-model [3], the development of a system is broken down into the development of each component of the system. After the design details of each component are determined, the component design is validated, followed by a system validation phase to ensure the overall system-level development target is reached. In this development process, component requirements play a crucial role since they guide component design and provide criteria for component validation. This is also true in the product development process for noise reduction. However, without a systematic computation method, the component targets would not correlate well with the system-level noise reduction targets and thus cannot guarantee the success of the overall development, as shown in [4]. Research on deriving the component requirements based on the overall system noise requirements can

be traced back to the 1990s, to the authors' best knowledge. In [5–7], the system noise is expressed as the summation of the noise contribution of all transfer paths, which are considered decoupled from each other (as illustrated in Figure 1 (c)). The most dominant transfer paths are assigned upper noise limits or reduction targets. However, these targets are not further decomposed onto the component level, since the relationship between the transfer path dynamics and the component dynamics are not modeled. To solve this problem, researchers in [2, 8] characterize the component dynamics as transmissibility and coupled them to get the transmissibility of the whole transfer path (see Figure 1, (b)). The component transmissibility of components is expressed as the ratio of acceleration between the active and passive side, which is, however, dependent on the dynamics of other components and thus not a property of the isolator element itself. Coupling the transmissibility of components may largely affect the prediction accuracy once some components on the transfer paths are redesigned. A more accurate coupling method is the Four Pole theory, based on which Münster et al. [9] modeled the transfer of road-caused tire vibration to the steering wheel. The upper and lower limiting curves of steering column dynamics are then derived analytically, which can assure that the vibration at the steering wheel is lower than a limit value. However, coupling the component dynamics based on their transmissibility or with the Four Pole method is only able to couple the components in series connections (as in Figure 1 (b)). This limits their application for more complex systems, where multiple connected transfer paths exist (as in Figure 1, (d)). A more general method for coupling components is the Frequency-Based Substructuring (FBS) method [10, 11], which allows arbitrary connections of components.

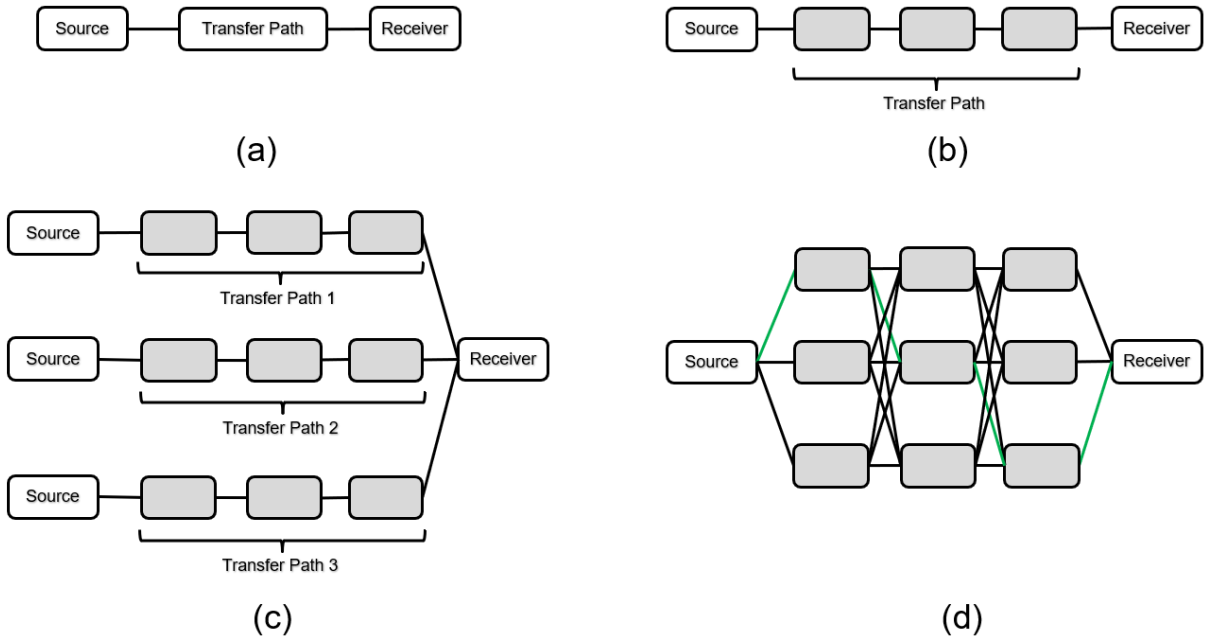

Figure 1: Propagation of structure-borne noise in mechanical systems of different complexity. (a) The general source-transfer path-receiver model for vibration and noise propagation problems. (b) The transfer path is decomposed into components. Each grey box indicates a component on the transfer path. (c) Parallel transfer paths contribute together to the noise perceived by the receiver. (d) The more general propagation problem, where multiple transfer paths intersect with each other. One of the transfer paths is marked in green as an example.

In research mentioned above, the noise contribution of each path is assumed to be the product of excitation force (or acceleration as in [6]) and the transmissibility of the transfer path based on the Transfer Path Analysis (TPA). This is later categorized as classical TPA in [12]. Here the interface force between the source structure and the transfer path is used as excitation force, which would in general be different once the dynamics of the transfer path are changed, for example due to the new design of a certain component on the transfer path. The noise prediction would be inaccurate if this excitation force is not updated for the new transfer path due to, e.g., the lack of physical prototype. Instead of this interface force, van der Seijs [12] characterizes the excitation of the source structure with the so-called *block force*, which is the interface force

between the excitation source structure and the fixed boundary condition, if the source were decoupled from the original mechanical system and fixed rigidly. This force is only a property of the source structure itself and is independent of the dynamics of the transfer paths. Based on the block force, the block force TPA can predict the system response accurately after redesigning a certain component without having to measure the source excitation again.

Based on the FBS method and block force TPA, Häußler et al. [13] developed an optimization process to find the best rubber isolators for the noise reduction of an example structure from the given rubber isolator candidates. However, this optimization is limited by the isolator candidates given a priori. Also, this could be computationally expensive if many market available isolator products are to be considered candidates. In [14], the stiffnesses of rubber mounts are used as design variables and are optimized so that the minimum vibration level is reached. However, the optimization of the rubber isolator only provides a single target value of isolator stiffness. It could be unrealistic for isolator suppliers to reach this exact value, especially when the target stiffness value of different directions must all be met.

Instead of only finding a single optimum design, the solution space method [15] computes the admissible range of design variables and thus provides more realistic requirements for component suppliers. The complete design space is sampled randomly, and the performance of each sample design is evaluated against the development requirement. By plotting good designs and bad designs together, one can easily identify the *solution space* to a design problem, which can help identify the admissible range of each design variable. As long as the values of design variables of the final design are within the admissible range corresponding to the computed solution spaces, the development requirement is guaranteed to be fulfilled. The solution space method provides a systematic design method to account for multi-disciplinary design targets for systems with high complexity and strong nonlinearity. It also increases the flexibility and robustness of the development process. By defining admissible intervals for each design variable, possible designs are limited to a high-dimensional, box-shaped solution space, which is smaller than the original solution space and thus could lead to a large sacrifice of design possibilities. One approach to alleviate this problem is to enlarge the design spaces of some design variables (early-decision variables) by compensating for others (late-decision variables) [16]. Another way to enlarge the solution space is to define the solution space as polygon instead of box [17].

This paper aims to compute component requirements for the vibrating mechanical systems with multiple connected transfer paths in order to provide clear targets for component development or product selection, so that the structure-borne noise of the whole system is lower than a given level. To do so, first the system dynamics are modeled with the FBS method and block force TPA. Then, based on this system model, the admissible area of component dynamics, in this paper the rubber mount stiffness as an example, is computed using the solution space method. The whole process is detailed in Section 2. In Section 3, the proposed process is applied to a practical example from the automobile industry. Some conclusions and an outlook for further work are given in Section 4.

2 Method

2.1 Overall process

At the beginning of the development process for engineering systems, the requirements on the overall system performance are defined [18]. For vibrating mechanical systems, it is desirable for the noise to be kept below a certain level. This system-level requirement is accomplished by properly designing isolation elements in the component development phase. The requirement on this component development can be derived from the system-level requirement in two steps: system modeling and solution space computation (see Figure 2).

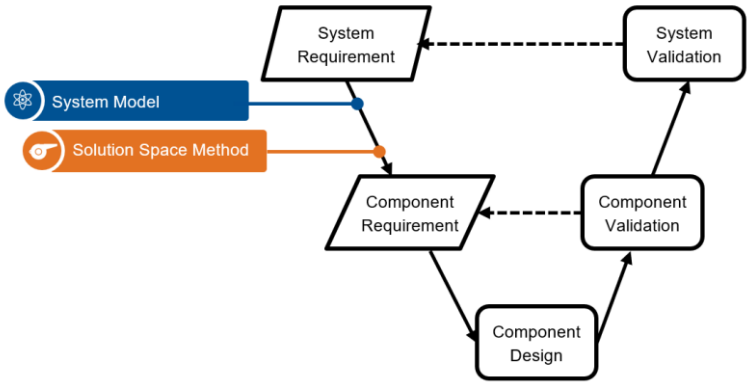

Figure 2: V-model with integrated steps for component requirement computation

Once the component requirements are determined, they can be used to guide the component design process and evaluate the performance of a certain design in the component validation phase. Alternatively, existing products in the market that fulfill the component requirements can also be used instead of designing new components. The remainder of this paper focuses on computing the component requirements on a rubber mount, since that is the most used isolation element for mechanical systems.

2.2 System modeling

2.2.1 Rubber mount model

The rubber mount is usually softer than the neighboring structures and provides a flexible connection. A commonly used simplified dynamic model assumes that the rubber mount connects two structures in each spatial direction as a spring [19], whose stiffness is complex in general and can vary over frequency. The coupling stiffness between different directions is neglected (see Figure 3).

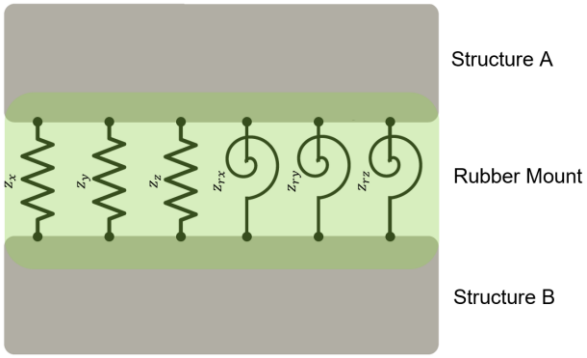

Figure 3: Simplified dynamic model of rubber mounts

With this simplification, the admittance matrix of a rubber mount $\boldsymbol{Z}_{RM}$ reads

$$\boldsymbol{Z}_{RM} = \begin{bmatrix} \boldsymbol{z} & -\boldsymbol{z} \\ -\boldsymbol{z} & \boldsymbol{z} \end{bmatrix} \text{ with } \boldsymbol{z} = \begin{bmatrix} z_x & 0 & 0 & 0 & 0 & 0 \\ 0 & z_y & 0 & 0 & 0 & 0 \\ 0 & 0 & z_z & 0 & 0 & 0 \\ 0 & 0 & 0 & z_{rx} & 0 & 0 \\ 0 & 0 & 0 & 0 & z_{ry} & 0 \\ 0 & 0 & 0 & 0 & 0 & z_{rz} \end{bmatrix} \tag{1}$$

where z_x, z_y and z_z represent the stiffness of the rubber mount in translational directions. z_{rx}, z_{ry} and z_{rz} indicate the stiffness in rotational directions.

2.2.2 Coupling the rubber mounts with other components

Frequency-Based Substructuring (FBS) is known to be able to couple the admittance matrix of an arbitrary number of components (usually referred to as substructures in the framework of FBS) with arbitrary connection relationships to each other. The admittance of the whole transfer path $\widetilde{\boldsymbol{Y}}$ can be computed based on the admittance of each component $\boldsymbol{Y}_i$ and their topological connection relationship

$$\widetilde{\boldsymbol{Y}} = (\boldsymbol{I} - \boldsymbol{Y}\boldsymbol{B}^T(\boldsymbol{B}\boldsymbol{Y}\boldsymbol{B}^T)^{-1}\boldsymbol{B})\boldsymbol{Y} \tag{2}$$

Here, $\boldsymbol{Y}$ is the admittance matrix of the transfer path in the unassembled state, which can be constructed by putting the admittance matrix of each component $\boldsymbol{Y_i}$ as block matrix onto the diagonal. $\boldsymbol{I}$ is the unit matrix. The matrix $\boldsymbol{B}$ is the so-called 'signed Boolean matrix', which enforces the compatibility condition at the coupling

$$\boldsymbol{B}\boldsymbol{u} = \boldsymbol{0} \tag{3}$$

The admittance matrix $\boldsymbol{Y}_i$ of each substructure can be determined experimentally or through FE simulation for a certain design. During the solution space computation, the noise of the system with certain rubber mount stiffnesses is to be predicted before any physical or virtual prototype is available. Therefore, the admittance matrix of rubber mount $\boldsymbol{Y}_{RM}$ cannot be measured or simulated. Instead, it must be constructed based on the impedance matrix $\boldsymbol{Z}_{RM}$ in Equation 1. However, $\boldsymbol{Z}_{RM}$ is singular according to Equation 1 and thus cannot be directly inverted to get the admittance $\boldsymbol{Y}_{RM}$. This problem is solved by adding virtual mass to the impedance matrix [11, 20]

$$\widehat{\boldsymbol{Y}}_{RM} = \left(\widehat{\boldsymbol{Z}}_{RM}\right)^{-1} \text{ with } \widehat{\boldsymbol{Z}}_{RM} = \boldsymbol{Z}_{RM} - \omega^2\boldsymbol{M} \tag{4}$$

$\boldsymbol{M}$ is a diagonal matrix of virtual masses. $\widehat{\boldsymbol{Y}}_{RM}$ and $\widehat{\boldsymbol{Z}}_{RM}$ indicate the admittance and impedance matrix of rubber mounts with the virtual mass. The added virtual mass should be considerably small so that the rubber mount dynamics are not changed considerably. The resonance frequency of the rubber isolator with virtual mass should be much higher than the frequency of interest of the noise prediction.

The local coordinate system of a rubber mount could, in general, be different from the global coordinate system due to the orientation of the rubber mount in the mechanical system. In this case, the impedance matrix $\widehat{\boldsymbol{Y}}_{RM}$ must be transferred to the global coordinate system by pre- and post-multiplying it with a rotation matrix $\boldsymbol{R}$ to account for the spatial orientation of the rubber mount

$$\boldsymbol{Y}_{RM} = \boldsymbol{R}\widehat{\boldsymbol{Y}}_{RM}\boldsymbol{R}^T \tag{5}$$

Other components on the transfer path are not redesigned in the scope of this research. Their admittance matrixes only need to be measured or simulated once. With the help of the virtual point transformation technique [12], the interfaces of these components to the rubber mounts are simplified as virtual points, each of which has six DoFs, and thus are compatible with the isolator model in Section 2.2.1. By inserting the admittance matrix of the rubber mounts and other components on the transfer path into Equation 2, one obtains the admittance matrix of the whole transfer path $\widetilde{\boldsymbol{Y}}$ for the proposed rubber mount stiffness z_i.

2.2.3 Structure-borne noise prediction

Once the admittance matrix of the transfer path is determined, the system response can be computed based on the block force TPA as [12]

$$\boldsymbol{p}_3^B(\omega) = -\boldsymbol{Y}_{32}^{AB}(\omega)\boldsymbol{f}_2^{bl}(\omega) \tag{6}$$

In this research, the system performance is evaluated with the sound pressure $\boldsymbol{p}_3^B$ instead of displacement $\boldsymbol{u}_3^B$ as in the original framework in [12]. $\boldsymbol{Y}_{32}^{AB}$ represents the admittance matrix of the acoustic transfer

function between the excitation force of the source structure $\boldsymbol{f}_2^{bl}$ and sound pressure $\boldsymbol{p}_3^B$ at the receiver. $\boldsymbol{Y}_{32}^{AB}$ is computed by coupling all the components on the transfer path as introduced in Section 2.2.2. The block force $\boldsymbol{f}_2^{bl}$ can be measured either by constraining the source structure rigidly, or in-situ.

2.3 Computing component requirements with Solution Space Engineering

The method for solution space computation is introduced in [15, 21]. Here, only the basic definitions and algorithms are repeated.

For a typical design task, the design requirements are formulated for the quantities of interest $\boldsymbol{z}$, which represent the features used to evaluate the success of the design. The requirements are usually formulated as value intervals that the system response $\boldsymbol{z}$ needs to fulfill

$$\boldsymbol{z_l} \leq \boldsymbol{z} \leq \boldsymbol{z_u} \tag{7}$$

Assuming there are p design variables for a design problem, a certain design is represented by the vector $\boldsymbol{x} = (x_1, x_2, .. x_p)$ with x_i representing the value of each design variable. Usually, each design variable is only allowed to vary between a certain upper and lower limit

$$x_i^l \leq x_i \leq x_i^u \tag{8}$$

The set of all possible designs is called *design space*. The mapping function

$$\boldsymbol{z} = f(\boldsymbol{x}) \tag{9}$$

represents the relationship between the design variables $\boldsymbol{x}$ and the quantities of interest $\boldsymbol{z}$. The designs in the complete design space are sampled using random sampling. The performance of each sampling design is then evaluated with the mapping function in Equation 9 against the design requirement in Equation 7. The designs that fulfill the design requirement are called *good designs*. Otherwise, they are *bad decisions.* The set of all good designs is called *solution space*. A slice of solution space can be visualized by plotting the good and bad designs of two arbitrary design variables in a 2D plot. An arbitrary number of plots can be generated to check the pair-wise combination of any two design variables.

If the design variables are the characteristics of a component, it's usually desired that the design of each component is decoupled by assigning each design variable an admissible interval $[x_i^l, x_i^u]$. The overall system requirement can be reached as long as the value of each design variable stays inside the corresponding intervals through proper component design. These intervals form box-shaped solution spaces, also called *solution boxes* (see Figure 4), which are a subset of the original total solution space. In this way, further design activity for each design variable can be decoupled. Algorithms to maximize the solution boxes can be found in [15].

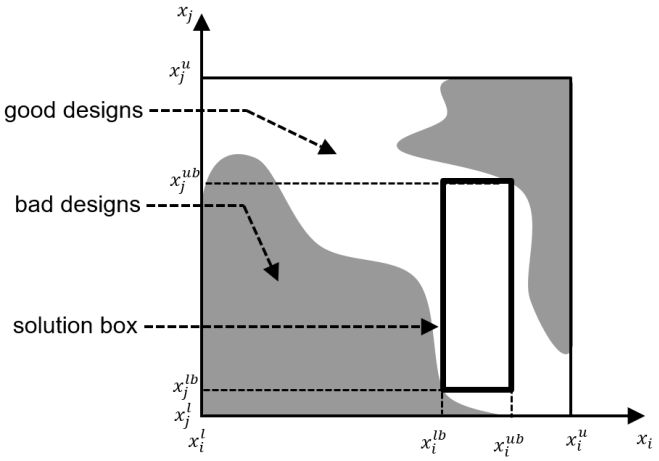

Figure 4: Design space and solution space

3 Case study: Electrical compressor

3.1 Design problem

The proposed method is exemplified by a long-range battery electric vehicle (BEV) as an industry relevant example based on the previous research [22]. This paper focuses on the structure-borne noise in the passenger cabin caused by the electric compressor of the vehicle air conditioning system. This would be especially annoying for electric vehicles if the compressor mounting is not properly designed, since the masking effect of the internal combustion engine (ICE) is missing. For confidentiality reasons, the actual vehicle and exact value of results cannot be shown in this paper. The topological setup of this mechanical system is illustrated in Figure 5. In this application example, the compressor is mounted through the vibration isolation of the first level, which consists of four rubber mounts, on a carrier structure. The carrier is further mounted on the subframe through the vibration isolation of the second level, which consists of three rubber mounts. The vibration is transferred through the subframe over the car body to the cabin, which is then transferred into noise perceived by the driver's ear. The transfer path from isolation level 2 to the driver's ear is considered as one single component and is marked as 'vehicle' in Figure 5. All rubber mounts are located at different positions and have different orientations.

Since the rubber mounts play an important role in the vibration reduction for the noise reduction in this application case, this paper aims to compute the admissible range of the rubber mount stiffness and use them as component requirements to help select the right product from candidate products existing in the market, so that the overall system-level requirements regarding structure-borne noise is fulfilled. In order to lower the complexity and cost of vibration isolation, the same rubber mount is assumed to be used at the different positions of each isolation level, while the rubber mounts can be different between both levels. The maximum rotational speed of the compressor (8600 rpm) is chosen to be the working condition in this case study.

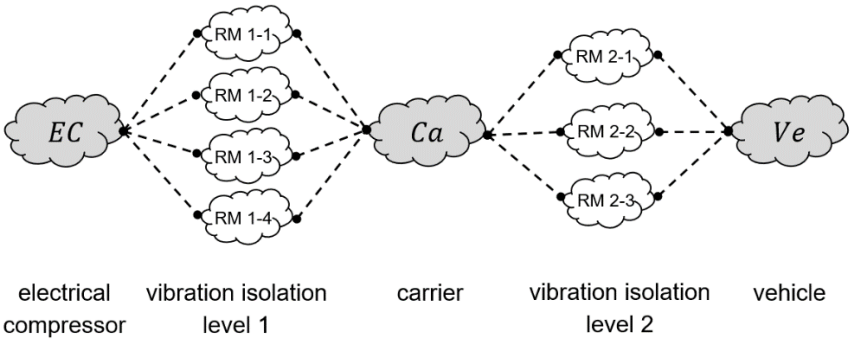

Figure 5: System topology of the compressor problem

3.2 System modeling

The admittance matrix of the compressor is computed analytically based on its mass and moment of inertia. The admittance matrixes of other components are measured experimentally. The dynamic stiffness of rubber mounts currently used in the vehicle is also measured experimentally for validation purpose. This measurement is conducted based on the rubber mount model introduced in Section 2.2.1. The admittance matrix of the transfer path in the uncoupled state $\boldsymbol{Y}$ reads

$$\boldsymbol{Y} = \begin{bmatrix} \boldsymbol{Y}_{EC} & & & & & & & & & & \\ & \boldsymbol{Y}_{RM\ 1-1} & & & & & & & & & \\ & & \boldsymbol{Y}_{RM\ 1-2} & & & & & & & & \\ & & & \boldsymbol{Y}_{RM\ 1-3} & & & & & & & \\ & & & & \boldsymbol{Y}_{RM\ 1-4} & & & & & & \\ & & & & & \boldsymbol{Y}_{Ca} & & & & & \\ & & & & & & \boldsymbol{Y}_{RM\ 2-1} & & & & \\ & & & & & & & \boldsymbol{Y}_{RM\ 2-2} & & & \\ & & & & & & & & \boldsymbol{Y}_{RM\ 2-3} & & \\ & & & & & & & & & \boldsymbol{Y}_{Ve} \end{bmatrix} \quad (10)$$

Note that the admittance matrices $Y_{RM\ 1-1}$ to $Y_{RM\ 1-4}$ are different since their installation orientations are different, although the same rubber mount product is supposed to be used. So is the isolation level 2 as well. The admittance matrix of the whole transfer path $\tilde{\boldsymbol{Y}}$ is then obtained by inserting $\boldsymbol{Y}$ into Equation 2 for coupling. The coupling is implemented in the vibes MATLAB Toolbox®.

The coupling results with the current rubber design are validated against the reference measurement, where the admittance matrix of the whole transfer path is measured directly in the assembled state of the vehicle. The transfer function between the first rubber mount of level 1 and the last rubber mount of level 2 is plotted in Figure 6. It can be seen that the system dynamics are accurately modeled compared to the reference measurement.

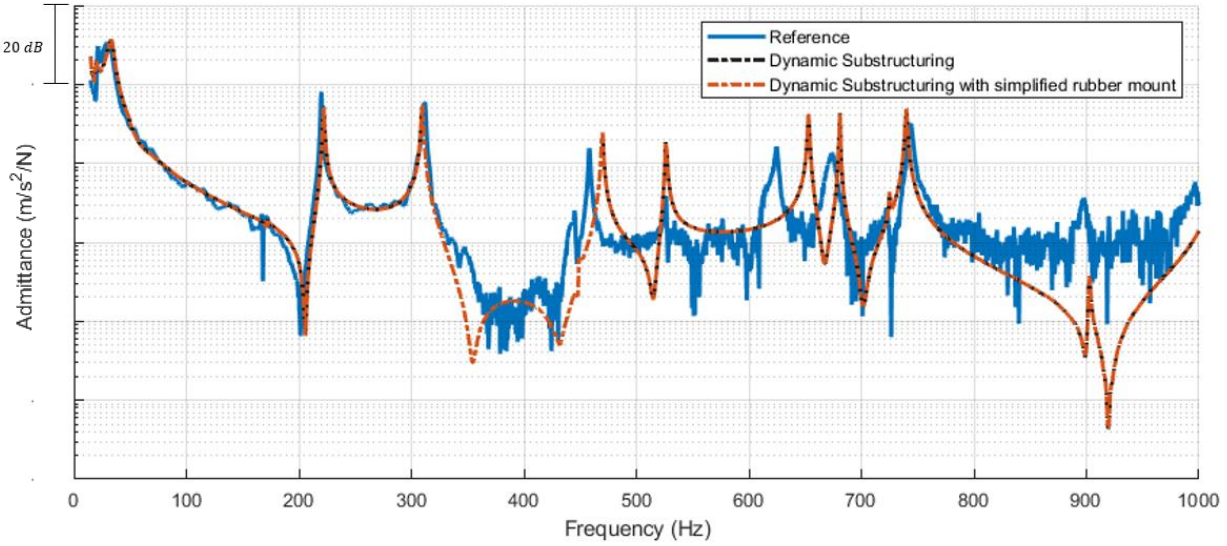

Figure 6: Admittance of the transfer path between rubber mount 1-1 and 2-3

Furthermore, the stiffness of the three rotational DoFs of all rubber mounts is set to zero for simplicity. Then the admittance matrixes of the rubber mounts are computed and again coupled with other components. According to Figure 6, this simplification does not lead to an obvious decrease in the modeling accuracy. Therefore, only the rubber mount stiffnesses in the three translational directions are used as design variables in the following, so the total number of design variables is smaller.

Then the noise level in the passenger car is predicted with the block force TPA method as introduced in Section 2.2.3. This is also implemented in the vibes MATLAB Toolbox®. The predicted sound pressure level is plotted in Figure 7. The direct measurement of structure-borne noise alone is difficult since the air-borne noise of the compressor is hard to completely insulate in operation. Therefore, no reference measurement data is available to validate the TPA prediction. Interested readers are referred to [22] for the validation of the total noise level, where the air-borne noise is included.

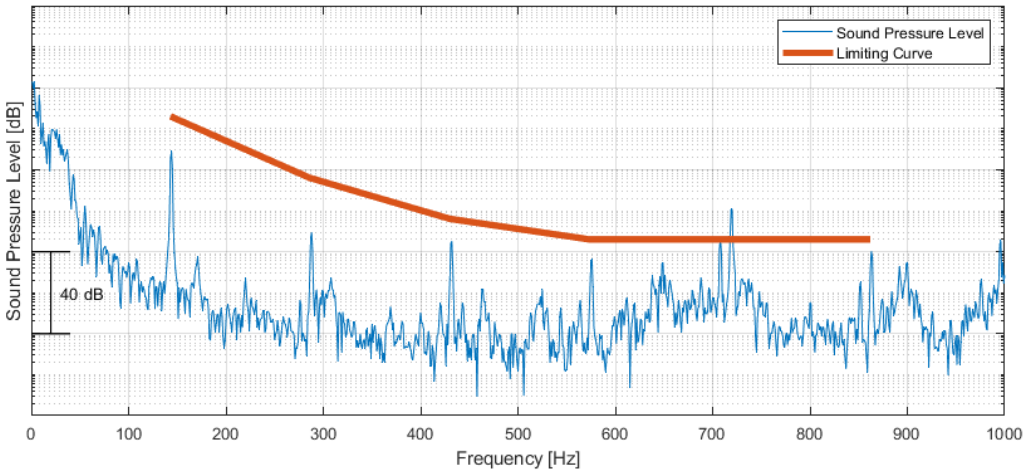

Figure 7: Sound pressure level in the cabin over frequency with the current design of rubber mounts

3.3 Component requirement computation

Based on the system model built in the last section, the component requirements are computed in two ways, with differences in details in the following.

3.3.1 Overall noise level as quantity of interest

In this section, the system-level requirements are defined as overall level of noise $P_{OA}(\boldsymbol{x})$ in the driver's ear

$$P_{OA}(\boldsymbol{x}) = \int_{\omega_{min}}^{\omega_{max}} \frac{|P(\omega,\boldsymbol{x})R_A(\omega)|}{P_0} \leq \hat{P}_{OA} \tag{11}$$

R is the A-weighting factor; $\hat{P}_{OA}$ is the target value of the overall noise; P_0 equals 2×10^{-5} Pa. The design variables are the stiffnesses of the rubber mounts in different directions for level 1 (z_{1x}, z_{1y}, z_{1z}) and level 2 (z_{2x}, z_{2y}, z_{2z}), see Figure 8.

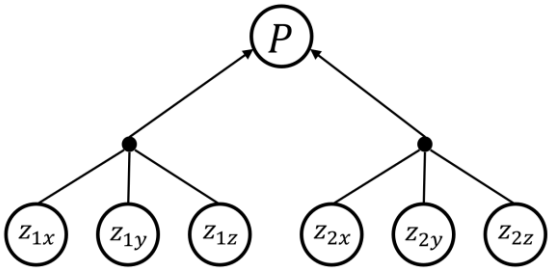

Figure 8: Dependency between overall noise level and rubber mount stiffnesses

In this research, 1000 sampling points are evaluated to generate each 2D plot of the solution space. And for each design the system response is evaluated over the frequency range from 100 Hz to 500 Hz, with 1 Hz as the frequency increment. This leads to a large computational burden, since the FBS and TPA must be conducted for each frequency. In order to speed up the computation of each solution space, a surrogate model is built based on neural network as the mapping function between rubber mount stiffnesses and overall noise level. 2000 sampling designs are generated randomly inside of the design space. These data are then imported into the commercial software ClearVU ® to train the neural network, which is used here to compute the solution space. The computed solution space can be seen in Figure 9, based on which the admissible range of each stiffness can be identified.

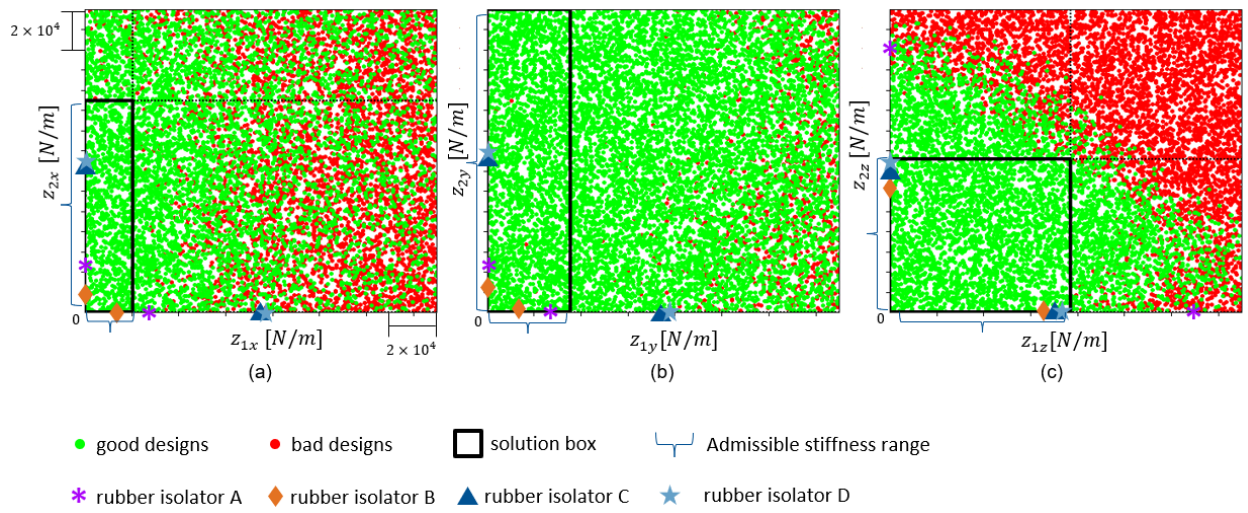

Figure 9: Solution space computed based on the overall noise level

Four rubber mounts existing in the market are used in this paper as candidates. They are marked as A, B, C, and D, respectively. Their dynamic stiffness is measured experimentally with the method proposed in [19]. As shown in Figure 14, their low frequency stiffnesses remain approximately unchanged up to 500 Hz and are used here to be compared with the admissible range. For the isolation level 1 (y-axis of plot a, b, and c in Figure 9), all candidates fit into the solution space, except for rubber isolator A. For level 2, only rubber isolator B is in the admissible range for all x, y, and z-directions (x-axis of plot a, b and c in Figure 9). For validation purposes, the rubber mount B is used for both levels and inserted into the system. The overall noise is reduced from $1.05\hat{P}$ of the original design to $0.81\hat{P}$ in decibel. The design target is reached.

3.3.2 Frequency-dependent sound pressure as quantity of interest

As the frequency increases, the damping due to the hysteresis effect of the rubber and resonance due to rubber mount inertia start to play a role, which makes the dynamic stiffness vary with frequency in general. In order to account for the frequency dependency of the rubber mount stiffness on frequency, the component requirement regarding the rubber mount is computed for different frequencies in this section. To do that, the system-level requirement must be defined for the corresponding frequencies in a priori. The system-level requirement is defined as a frequency-dependent upper limit curve for the sound pressure level

$$P(\omega, \boldsymbol{x}) \leq \hat{P}(\omega) \tag{12}$$

Due to the human sensitivity to the noise of different frequencies, the frequency-dependent target level of higher frequency is defined to be lower than the lower frequencies in this case study (see Figure 7). Unlike the case in Section 3.3.1, the solution space should be computed for each frequency of interest. Here, the solution space will be computed at the first order excitation frequency (143 Hz) and higher orders below 1000 Hz, since they are the frequencies with the highest noise levels within the frequency range of interest. As shown in Figure 7, the system requirement is not fulfilled with the current choice of rubber mounts.

The design variables are the rubber mount stiffnesses at each frequency, which are complex values in general due to damping. Thus, the imaginary part of the dynamic stiffness is used additionally as a design variable (see Figure 10). The computation of solution space is implemented in MATLAB®. Figure 11 shows the solution spaces computed for the first excitation order (143 Hz). Circles fit better to the solution space than solution boxes, thus the component requirements are defined as circular areas on the complex plane for each stiffness in this particular case. A dot in each diagram represents a design. The position of the design in the diagram corresponds to the values of the design variables shown on the diagram axes. The values for all other design variables are chosen randomly from within the circular region shown in the other diagrams. In

order to fulfill the overall system requirement, each stiffness must stay inside of the corresponding circle on the complex plane.

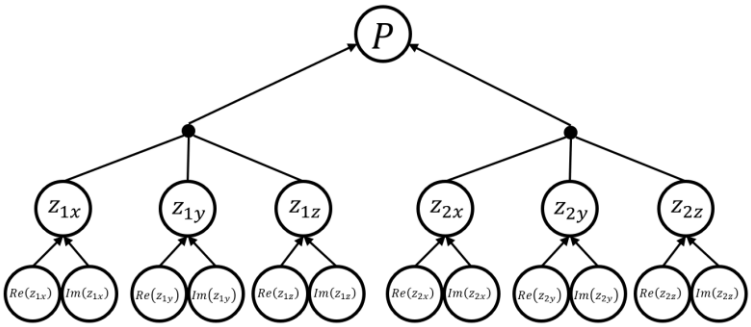

Figure 10: Dependency between sound pressure level and complex rubber mounts stiffnesses

If it is desired to relax the requirement on the stiffness in a particular direction, e.g., z_{1x}, its circle must be enlarged (see Figure 12). As a result, red points are seen in other circles, and the previous solution spaces are 'polluted' by bad designs. This means the fulfillment of component requirements can no longer guarantee the success of the development of the overall system.

By making the circle for z_{2z} smaller, all circles again only contain good designs, as can be seen in Figure 13, although the circle for z_{1x} is bigger than in Figure 11. This means that the solution spaces of all stiffnesses have mutual influence on each other. If the circle of a certain stiffness is desired, the solution space of other stiffnesses may become smaller. This may be compensated for by shrinking some other circles. Algorithms to find the biggest circle size, while balancing the size of different circles, are not in the scope of this research. In the following, the direct computation result of solution space is used without optimizing further. For 143 Hz, the solution space in Figure 11 is used as the final result, instead of the one in Figure 13.

The position of each solution space on the complex plane, and its size, depend on the system-level requirements and the dynamics of other components on the transfer path, which are in general frequency-dependent. So, the solution space also varies over frequency. The solutions space must be computed for all the frequencies of interest. For the computed solution space at one frequency, only the system response at this single frequency needs to be evaluated, thus the solution space computation is much faster than with the method in Section 3.3.1. However, the total time expense could be enormous, since the solution space must be computed at multiple frequencies.

In this case study, the solution space is further computed for higher orders of the base frequency. When the circles of each frequency are connected, an admissible area in the form of tubes is formed, as shown in Figure 14. All rubber mounts whose dynamic stiffness in the x-, y-, and z-direction all stay inside the tubes of level 1, can be used for level 1. This also applies to level 2. This ensures that the system noise level is lower than the limit value. The same rubber mount candidates are used as in Section 3.3.1. Their dynamic stiffnesses are compared to the component requirement in Figure 14.

In the lower frequency range, the four candidates can fulfill the requirement in all directions. For isolation level 1, the rubber mount B breaks out of the tube in the y-direction in the frequency range from 600 to 1000 Hz. The rubber mount A does not fulfill the component requirement near 800 Hz in the x- and y-direction. For isolation level 2, the rubber isolators A, C and D all break out of the tube in the y- and z-direction in the higher frequency range. Finally, rubber mounts C and D are selected for level 1 and B for level 2. The noise level with rubber isolator C for level 1 and B for level 2 is compared to the system requirement in Figure 15 as validation. The system requirement is fulfilled.

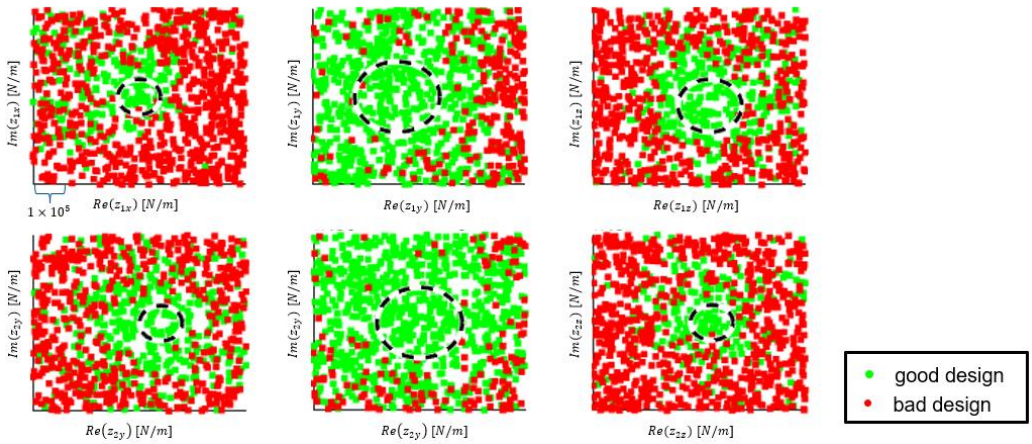

Figure 11: Initial candidate space representing admissible dynamics stiffnesses for rubber mounts 1 (top) and 2 (bottom) at f=143 Hz: good approximation of a solution space, as it includes only one bad design.

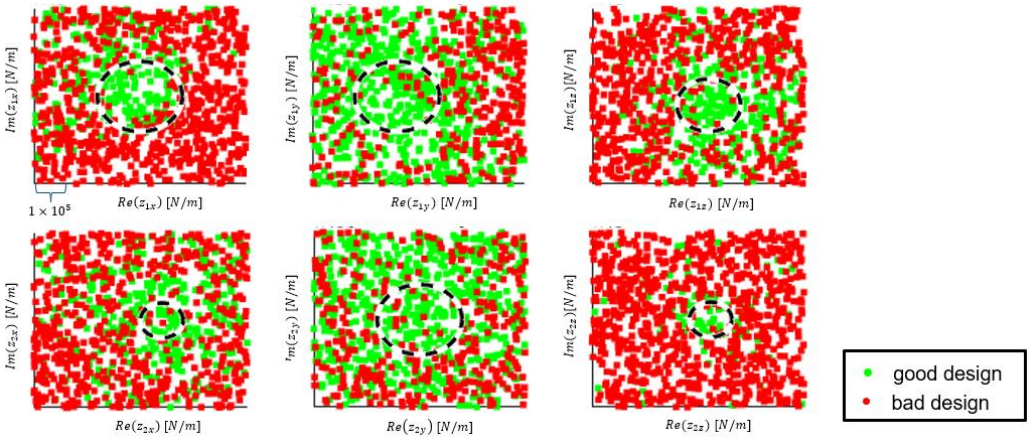

Figure 12: Extended candidate space with relaxed range for z_{1x}: bad approximation of a solution space, as many bad designs are included.

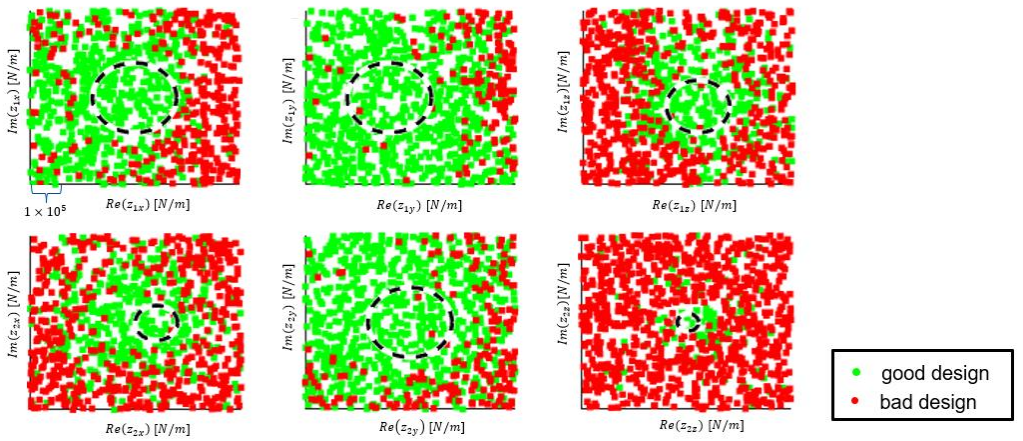

Figure 13: Final candidate space with relaxed range for z_{1x} and tightened range for z_{2z}: good approximation of a solution space, as only one design is included.

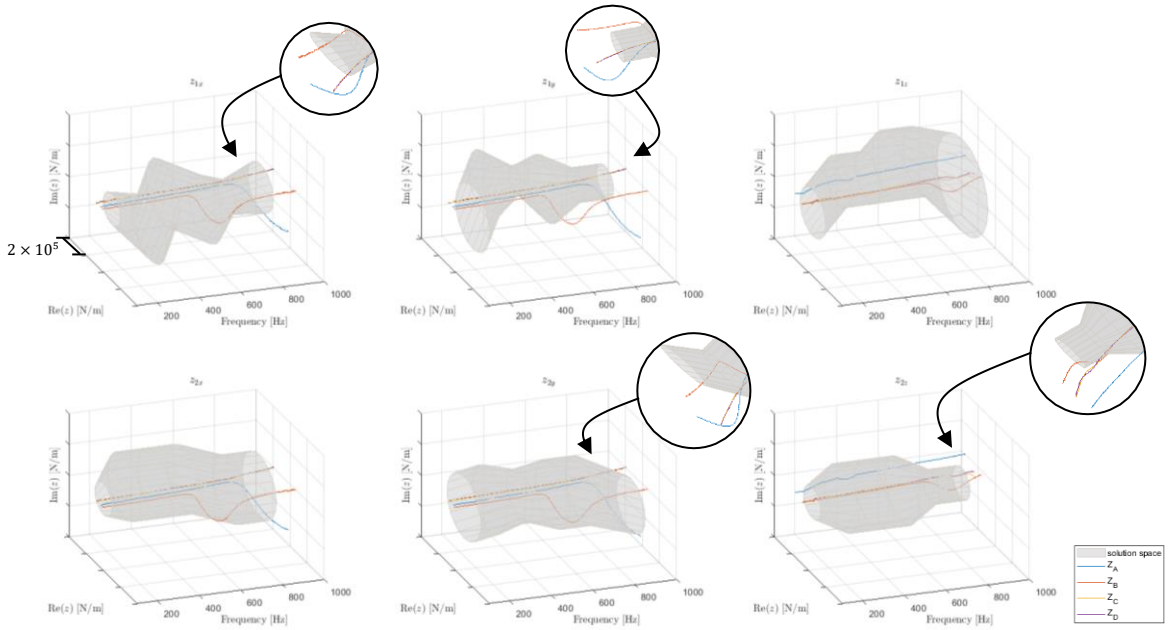

Figure 14: Permissible ranges (tubes) and rubber mount stiffnesses of existing bushings (lines)

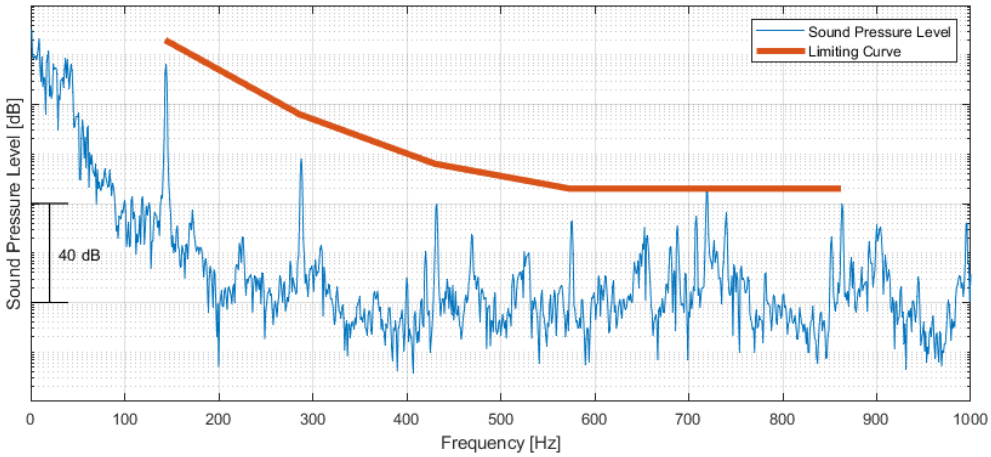

Figure 15: System performance realized (thin line) and limit (thick line)

4 Summary

This paper proposed a systematic method to derive component requirements quantitatively based on the system level noise target for the structure-borne noise problem where multiple transfer paths are connected. The proposed method consists of two steps: system modeling and solution space computation. Using the FBS and block force TPA method, the system noise can be accurately predicted for certain stiffness values of rubber mounts. Based on this system model and the desired system-level noise target, the admissible range of rubber mount stiffness is then computed using the solution space method, quantitatively.

In this paper, the proposed method is applied to the structure-borne noise caused by the electric compressor in an electric vehicle. Two ways to implement the proposed method are introduced, with the difference regarding the definition of quantity of interest and whether the change of the dynamic stiffness over frequency is considered. The first approach uses the overall noise level over a certain frequency range of interest as the quantity of interest. The system-level requirement is defined as an upper limit of the overall

noise level. The stiffness of the rubber mount, which is assumed to be a real value and constant over frequency, is used as the design variable. This assumption is mainly valid for the lower frequency range.

For applications where the noise of the broader frequency range is of interest, and thus the change of dynamic stiffness due to damping and inertia are not negligible, the second approach provides the possibility of defining a limiting curve to the noise level over frequency. The solution space is computed for each frequency of interest. Due to the damping effect of the rubber, the dynamic stiffness of the rubber mount in general is a complex value. Thus, the imaginary part of the dynamic stiffness is additionally added here as a design variable. The component requirements are set to be circular areas on the complex plane, instead of boxes or polygons as in previous research on solution space engineering.

If the design task mainly focuses on the noise in the lower frequency range, where the assumption of frequency-independent rubber mount stiffness is acceptably valid, the first method would be preferable regarding computational cost. Otherwise, the second method should be applied, where the complex dynamic behavior of the rubber mount can be accurately accounted for in a larger frequency range. Although the time expense of each computation of solution space is smaller than the first approach, the total time expense could be higher, since the solution space must be computed for multiple frequencies.

The process for target cascading proposed in this research provides a systematic method for the noise reduction of complex mechanical systems. It provides clear component targets to enable product development regarding noise reduction in a top-down manner. No assumption is made on the rubber mount geometry or material during the system modeling or solution space computation. Thus, the computed solution space provides solution-neutral component requirements. All the designs that can fit into the solution space will guarantee the fulfillment of the system level requirement.

In the case study there is only one source (compressor) and the requirement is only cascaded down from the system level to the component level. For more complex applications, the proposed method can easily be extended to account for multiple sources (e.g., engine, road, etc.) and more structural hierarchies (e.g., subsystem, part, etc.). Furthermore, multi-disciplinary requirements can be integrated into the existing framework of the proposed method, provided that the relationship between the design variables and the other requirements are modeled quantitatively. In addition to the requirement regarding noise, rubber mounts must also fulfill further requirements. In the practical application, the motor must be supported with enough stiffness to limit its displacement in various driving maneuvers. This requirement is generally in conflict with noise reduction, where softer rubber mounts are normally beneficial. By adding additional requirements regarding minimum static stiffness, the solution space would be smaller and thus further limit rubber mount choice. If there are still multiple rubber mount products that can fulfill the component requirements, one can select the cheapest or lightest product as the final decision.

As shown in this research, the solution spaces of different rubber mount stiffnesses influence each other. Only one possible solution space result is shown in this paper. There could also exist other solution spaces that can ensure the fulfillment of the system noise target, although these solution spaces have different positions on the complex plane and sizes than the solution spaces shown in this paper. Algorithms to maximize the solution spaces and balance different circle sizes are to be developed in future work.

Acknowledgments

The authors would like to thank the Zeidler-Forschungsstiftung for funding this research.

References

[1] P. Zeller and others, *Handbuch Fahrzeugakustik*. Springer, 2009.

[2] T. Tousignant, K. Govindswamy, D. Tomazic, G. Eisele, and P. Genender, “NVH target cascading from customer interface to vehicle subsystems,” *SAE Technical Paper*, 2013.

[3] V. D. Bhise, *Automotive product development: A systems engineering implementation*. CRC Press, 2017.

[4] M. Ambardekar, and N. Solanki, "Performance cascading from vehicle-level NVH to component or sub-system level design," *SAE Int. J. Veh. Dyn., Stab., and NVH*, vol. 1, 2017-26-0205, pp. 58–65, 2017.

[5] T. Mori, A. Takaoka and M. Maunder, "Achieving a vehicle level sound quality target by a cascade to system level noise and vibration targets," in *SAE 2005 Noise and Vibration Conference and Exhibition*, 2005.

[6] P. J. van der Linden, K. Wyckaert and H. van der Auweraer, "Modular vehicle noise and vibration development," in *INTER-NOISE 2001-ABSTRACTS FROM INTERNATIONAL CONGRESS AND EXHIBITION ON NOISE CONTROL ENGINEERING*, 2001.

[7] P. W. Zeng, "Target setting procedures for vehicle powerplant noise reduction," *Sound and Vibration*, vol. 37, no. 7, pp. 20–23, 2003.

[8] B. Bergen, J. A. Chavan and K. van de Rostyne, "Target setting for vibration transmission through driveline components based on on-vehicle and on-bench evaluation," in *Automotive Acoustics Conference 2019*, 2020, pp. 109–121.

[9] M. Muenster, M. Lehner, and D. Rixen, "Requirement derivation of vehicle steering using mechanical four-poles in the presence of nonlinearities," *Mechanical Systems and Signal Processing*, vol. 155, p. 107484, 2021.

[10] D. de Klerk, D. J. Rixen, and S. N. Voormeeren, "General framework for dynamic substructuring: history, review and classification of techniques," AIAA Journal, vol. 46, no. 5, pp. 1169–1181, 2008.

[11] M. S. Allen, D. Rixen, M. van der Seijs, P. Tiso, T. Abrahamsson, and R. L. Mayes, *Substructuring in engineering dynamics*: Springer, 2020.

[12] M. van der Seijs, "Experimental dynamic substructuring: Analysis and design strategies for vehicle development," 2016.

[13] M. Haeussler, D. C. Kobus, and D. J. Rixen, "Parametric design optimization of e-compressor NVH using blocked forces and substructuring," *Mechanical Systems and Signal Processing*, vol. 150, p. 107217, 2021.

[14] A. El Mahmoudi, U. S. Paracha, and D. Rixen, "Design optimization of joint parameters using Frequency Based Substructuring," *Proc. Appl. Math. Mech.*, vol. 19, no. 1, e201900454, 2019.

[15] M. Zimmermann, and J. E. von Hoessle, "Computing solution spaces for robust design," *Int. J. Numer. Meth. Engng.*, vol. 94, no. 3, pp. 290–307, 2013.

[16] M. E. Vogt, F. Duddeck, M. Wahle, and M. Zimmermann, "Optimizing tolerance to uncertainty in systems design with early-and late-decision variables," *IMA Journal of Management Mathematics*, vol. 30, no. 3, pp. 269–280, 2019.

[17] H. Harbrecht, D. Tröndle, and M. Zimmermann, "Approximating solution spaces as a product of polygons," *Structural and Multidisciplinary Optimization*, vol. 64, no. 4, pp. 2225–2242, 2021.

[18] M. Zimmermann, and O. de Weck, "Formulating Engineering Systems Requirements," in *Handbook of Engineering Systems Design*: Springer, 2022, pp. 1–52.

[19] M. Haeussler, S. W. Klaassen, and D. J. Rixen, "Experimental twelve degree of freedom rubber isolator models for use in substructuring assemblies," *Journal of Sound and Vibration*, vol. 474, p. 115253, 2020.

[20] A. E. Mahmoudi, D. J. Rixen, and C. H. Meyer, "Comparison of different approaches to include connection elements into frequency-based substructuring," *Exp Tech*, vol. 44, no. 4, pp. 425–433, 2020.

[21] L. Graff, H. Harbrecht, and M. Zimmermann, "On the computation of solution spaces in high dimensions," *Structural and Multidisciplinary Optimization*, vol. 54, no. 4, pp. 811–829, 2016.

[22] M. Häußler, "Modular sound & vibration engineering by substructuring," Universität München, 2021.